IEEE Access
Multidisciplinary | Rapid Review | Open Access Journal

Received June 6, 2019, accepted June 14, 2019, date of publication June 19, 2019, date of current version July 9, 2019.

Digital Object Identifier 10.1109/ACCESS.2019.2923657

Fault Feature Extraction of Reciprocating Compressor Based on Adaptive Waveform Decomposition and Lempel-Ziv Complexity

YOUFU TANG AND FENG LIN
Mechanical Science and Engineering Institute, Northeast Petroleum University, Daqing 163318, China

Corresponding author: Youfu Tang (tang_youfu210@163.com)

This work was supported in part by the Natural Science Foundation in China under Grant 51505079 and in part by the University Nursing Program for Young Scholars With Creative Talents in Heilongjiang Province under Grant UNPYSCT- 2015078.

ABSTRACT The multi-source impact signal of reciprocating compressor often represents nonlinear and non-stationary. For this reason, the fault features of the signal are difficult to quantitatively describe using conventional signal processing methods. In this paper, a novel adaptive waveform decomposition method was proposed to convert the strong non-stationary multi-component signal into stationary single-component signal. Subsequently, the signal was denoised with threshold-based mutual information to protect from being interfered by the noise. Finally, to measure the nonlinearity of reciprocating compressor signals in four states (normal valve sheets, gap valve sheets, fractured valve sheets, and bad spring), the normalized Lempel-Ziv complexity indexes were employed. The results reveal that the proposed method is capable of extracting the different faults states of reciprocating compressor accurately, which supplies a measure of fault diagnosis and maintenance strategy for the reciprocating compressor.

INDEX TERMS Adaptive waveform decomposition, Lempel-Ziv complexity, reciprocating compressor, feature extraction, fault diagnosis.

I. INTRODUCTION

Reciprocating compressors are vital to the oil and chemical production. However, due to its more complex structure and motion, and the larger number of wearing parts, it is more difficult to diagnose than the rotating machines [1]. In various monitoring methods of reciprocating compressor, the vibration analysis method is the most widely used for its convenience in testing and its sensitivity to mechanical failure. It is generally known that in the field of mechanical fault diagnosis, the feature extraction method of vibration signal is continuously optimized with the advancement of signal processing technology. Many advanced fault feature extraction methods have been extensively studied [2]–[4]. However, owing to many internal excitation sources in reciprocating compressors, the monitored vibration signal of reciprocating compressor gas valve usually refers to a multi-source impact property, being typically nonlinear and non-stationary. Conventional signal processing techniques based on the assumption that the signal is stationary and linear might extract some false features when applied to the non-stationary signal [5]. Accordingly, features of reciprocating compressor are difficult to extract effectively.

Modern signal processing technique based on time-frequency analysis can effectively process the non-stationary multi-component signals. Several signal decomposition methods show the advantage of simplifying and processing multi-component signals. In recent years, a series of signal decomposition theories and techniques have been developed and widely used in various disciplines and engineering fields (e.g. Fourier transform [6], short-time Fourier transform [7], wavelet transform [8], Second-generation wavelet transform [9], multi-wavelet transform [10], chirplet transform [11] and atomic decomposition [12]). All of them are based on the basic function expansion of the inner product transform principle, performing the similarity measure between the signal and the basis function. The typical fault signals of rotating machinery with obvious

The associate editor coordinating the review of this manuscript and approving it for publication was Pia Addabbo.

waveform features (e.g. harmonic waveforms of rotor system faults, modulation waveforms of rolling bearing faults, and single-sided oscillation attenuation waveforms of gear faults) are well consistent with the decomposition results. Thus, modern signal decomposition techniques have significant application effect on fault feature extraction of rotating machinery.

However, for the reciprocating machinery, the vibration signal represents strong nonlinearity, non-stationarity and multi-source impact, so it is unlikely to adapt all waveform features using one or several given basis functions. In the absence of sufficient prior knowledge, if a fixed basis function is employed for signal decomposition, erroneous information will be generated, and the physical meaning will be unclear. Feature information sufficient to identify the fault is difficult to extract. In recent years, some adaptive signal decomposition methods, including empirical mode decomposition (EMD) [13], local mean decomposition (LMD) [14]and local characteristic-scale decomposition (LCD) [15], have been gradually proposed. Those methods are not required to predict the feature information contained in the analyzed signal, and they completely follow the waveform of the signal. Thus, it exhibits good adaptability in signal processing. Though many related achievements have been obtained in the field, they also have the following problems: 1) the magnitude of the feature amplitudes under different states are largely different, the real physical meaning is unclear, and the comparability is poor; 2) the feature amplitude under the same state may be significantly fluctuated with different samples, so the results exhibit poor repeatability and stability; 3) there may be different effects of noise interference on the accuracy of the results. Those problems are closely associated with the nonlinear dynamic characteristics of reciprocation compressor. It is an important prerequisite for fault diagnosis to judge and quantitatively describe the nonlinearity and evolution of reciprocating compressor in different states. For the nonlinear time series, some quantitative indicators (e.g. correlation dimension [16], Lyapunov exponents [17], entropy [18]–[22] and complexity [23]) have been well applied. Among them, the Lempel-Ziv complexity (LZC) has many good advantages to measure the complexity of time series arose from the nonlinear dynamics system. The more complex the time series, the larger the LZC value will be. Therefore, the LZC can be applied to quantitatively describe the fault feature of reciprocating compressor gas valve.

With the development of online testing technology, some real-time fault-diagnosis systems based on big data and machine learning algorithm are proposed [24]. There is an important theoretical significance and engineering value. However this method depend on complete condition monitoring system and cloud environment which could supply the big data of reciprocating compressor. Maybe some corporation petroleum and petrochemical enterprises do not have these conditions. Additionally, different fault samples are difficult to be obtained in daily monitoring, the identification of small sample is still a big problem for the machine learning algorithm. On the other hand, because of the influence of multi-source excitation, the sample space of fault feature represent strongly nonlinear, which will significantly increase the difficulty of classification. Therefore, effective fault feature vectors should be obtained first through signal processing techniques before recognition.

In order to improve the diagnosis accuracy of reciprocating compressor, effective and quantitative features should be extracted firstly. On one hand, the vibration signal of reciprocating compressor represents the complex feature of nonlinearity, non-stationarity and multi-source impact, many excitation information are mixed together, the typically and useful feature information may be not significant. On the other hand, the vibration signal of reciprocating compressor may be strongly influenced by background noise. For solving the above problems, an integration approach based on adaptive waveform decomposition (AWD) and Lempel-Ziv complexity (LZC) was proposed. Using the AWD method, the non-stationary multi-component signal of reciprocating compressor can be converted into a series of stationary single-component signal which are rich in useful feature information. The LZC method is applied to quantitatively describe the complexity of nonlinear signal and supply an effective feature. Therefore, both the AWD method and LZC algorithm have its own function in improving the diagnosis accuracy of reciprocating compressor, and the integration method of AWD and LZC will have the best effect. In summary, the main contributions of this paper are as follows

1) A novel AWD method is proposed which can adapt to the feature extraction of non-stationary signal with multi-components. The decomposition results only depend on the characteristics of the signal, and their physical meaning are more clear.

2) Based on the existing solution of Lempel-Ziv complexity (LZC), we developed a dynamic LZC algorithm. The dynamic LZC indicator of variation not only considers the global basic features of the signal, but also extracts local detail features.

3) In order to select the most useful waveform components that are rich in state information, the mutual information between each waveform component and the original signal were calculated. In the meantime, this method can reduce the interference of noise.

The rest of the paper is structured as follows: Section II introduces the architecture of the proposed solution; Section III presents the AWD algorithm process and its application in simulation signal and experimental data of reciprocating compressor; Section IV discuss the characteristics of LZC method on measure nonlinear time series; Section V extracts the fault feature of reciprocating compressor gas valve based on the integration of AWD and LZC method; and Section VI concludes the paper.

II. ARCHITECTURE

The proposed feature extraction of reciprocating compressor approach architecture is shown in FIGURE 1. The data

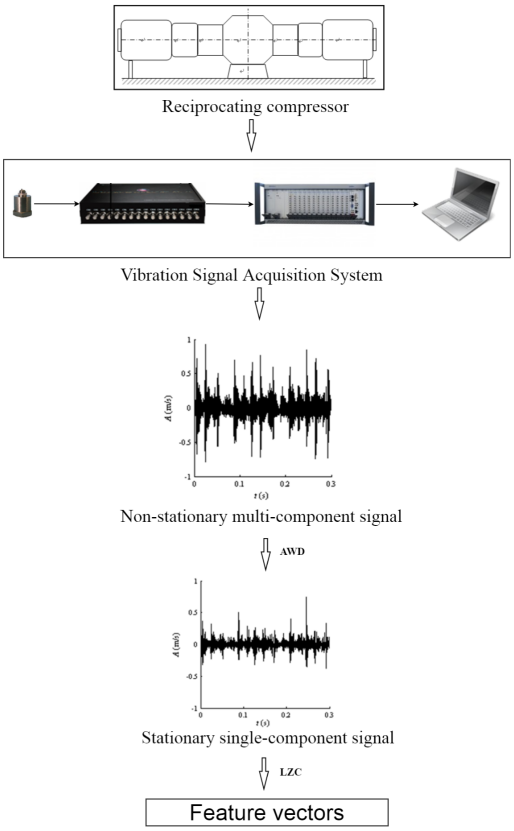

FIGURE 1. The proposed feature extraction of reciprocating compressor approach architecture.

analysis process runs in a offline environment. The proposed architecture has three main parts:

A. VIBRATION SIGNAL ACQUISITION

The working condition of each component in reciprocating compressor is not independent, and has some connections with other components. That is why the fault feature extraction of reciprocating compressor is so difficult in practice. For solving this problem, firstly, we select the test position and corresponding vibration data which is close to the component that need to be monitored.

B. NON-STATIONARY MULTI-COMPONENTS SIGNAL PROCESSING

The proposed AWD method can adaptively decompose the non-stationary multi-component signal into a series of stationary single-component signal without any prior mechanism knowledge of each component in reciprocating compressor. The useful fault feature information will be more prominent in the waveform component when the vibration signal changed with different component states.

C. NONLINEAR FEATURE DESCRIPTION

The LZC analysis of each waveform component will quantitatively describe the feature differences more significant. Therefore, the combination of the AWD method and the LZC method provides a solution strategy to identify the states of different components.

III. NON-STATIONARY MULTI-COMPONENT SIGNAL ANALYSIS BASED ON ADAPTIVE WAVEFORM DECOMPOSITION

A. ADAPTIVE WAVEFORM DECOMPOSITION ALGORITHM

Many test signals of machine usually contain various components from different excitations. Thus, to extract the feature of each component, the multi-component signal should be decomposed first. In the calculation of the conventional frequency and instantaneous frequency of the multi-component non-stationary signal, the signal can be finally reduced to the following two forms

$$x(t) = \sum_{k=1}^{\infty} c_k \sin(k\omega t + \theta_k) \tag{1}$$

$$x(t) = \sum_{k=1}^{N} a_k(t) \cos \phi_k(t) + R(t) \tag{2}$$

where $R(t)$ is the residual term.

The two formulas express frequency information in a superposition of multiple harmonic waveforms, which is much suitable for the multi-component signal of rotating machinery. However, the actual multi-component signal of reciprocating compressor do not exhibit harmonic waveform characteristics, and they are likely to consist of a limited number of other shape waveforms. Considering the efficiency, accuracy and frequency physical meaning of signal decomposition, the harmonic waveform combination is not consistent with the essential features of the signal. In this paper, a novel adaptive waveform decomposition (AWD) method was proposed to adapt to the feature extraction of non-stationary signal with multi-components.

$$x(t) = \sum_{m=1}^{N} s_m(t) + W(t) \tag{3}$$

where $s_m(t)$ denotes the mth waveform function contained in the original signal; $W(t)$ is the residual term. The implementation process is defined as:

1) Assuming that the discrete time series corresponding to the signal $x(t)$ is $\{x(i)|i = 1, 2, 3, \cdots, n\}$. Subsequently, according to equation (4), the local maxima n_1 in the signal $x(t)$ is found as the first layer extreme value sequence $\{p_1(k)|k = 1, 2, 3, \cdots, N_1\}$.

$$\begin{cases} x(i) \geq x(i-1) \\ x(i) \geq x(i+1) \\ x(i-1) \neq x(i+1) \end{cases} \tag{4}$$

2) A local mean $m(t)$, a local amplitude $a(t)$, and a local frequency can be given below

$$m(t) = \frac{1}{n_k} \sum_{i=1}^{n_k} x(t_i), \quad t_k \leq t < t_{k+1} \tag{5}$$

$$a(t) = \frac{x(t_k) + x(t_{k+1})}{2}, \quad t_k \le t < t_{k+1} \tag{6}$$

$$v(t) = \frac{1}{T(t)} = \frac{1}{t_{k+1} - t_k}, \quad t_k \le t < t_{k+1} \tag{7}$$

where n_k is the number of samples contained between the kth maximum and the $k+1$th maximum. The local frequency $v(t)$ represents the number of times completing the vibration in a unit of local time. It is used to measure the speed of local vibration, and the unit is still Hz.

The local amplitude $a_1(t)$, the local mean $m_1(t)$ and the local frequency $v_1(t)$ corresponding to the first-order extreme value sequence $p_1(t)$ are calculated by equation (5) to (7).

3) $a_1(t)$, $m_1(t)$, and $v_1(t)$ are smoothed using the moving average technique.

4) The local amplitude is de-averaged to yield the amplitude envelope curve $a_1'(t)$, which is expressed as

$$a_1'(t) = a(t) - m(t) \tag{8}$$

5) Likewise, the n_2 local maxima is found as the second layer $\{p_2(k)|k = 1, 2, 3, \cdots, N_2\}$ in first layer of extreme sequence $\{p_1(k)|k = 1, 2, 3, \cdots, N_2\}$, and smoothing and de-averaging processing are continued to yield the amplitude envelope curve $a_2'(t)$ following step 2), 3), 4).

6) Repeating the above steps until the m-th order extremum sequence $\{p_m(k)|k = 1, 2, 3, \cdots, N_m\}$ is found; when it satisfies $N_m \le 2$, the decomposition is ended.

According to the above method, $x(t)$ can obtain $m-1$ amplitude envelope curves $a_1'(t), a_2'(t), \cdots a_{m-1}'(t)$, so each component decomposed from $x(t)$ is obtained as follows.

$$\begin{cases} s_m(t) = a_{m-1}'(t) \\ s_{m-1}(t) = a_{m-2}'(t) - a_{m-1}'(t) \\ \vdots \\ s_1(t) = x - a_1'(t) \end{cases} \tag{9}$$

The mentioned decomposition process only depends on the characteristics of the signal $x(t)$ itself, and the local frequency of each components $s_1(t), s_2(t), \cdots s_m(t)$ does not depend on the harmonic form. Thus, the proposed AWD method exhibits good adaptability. According to the above description, a flow chart of the AWD algorithm is yielded, as shown in FIGURE 2.

B. SIMULATION ANALYSIS

It is known to all that different signal should require its appropriate signal processing technique. For the reciprocating compressor, the vibration signal typically represents the feature of nonlinearity, non-stationarity and multi-source impact. Before the application of proposed AWD method, we should verify the validity and applicability of AWD according to some simulation signal which have the similar features. In this way, we can easily justify the correctness of decomposition result by comparing with the original signal components defined in equation.

Before the application of proposed AWD method, we should verify the validity and applicability of AWD

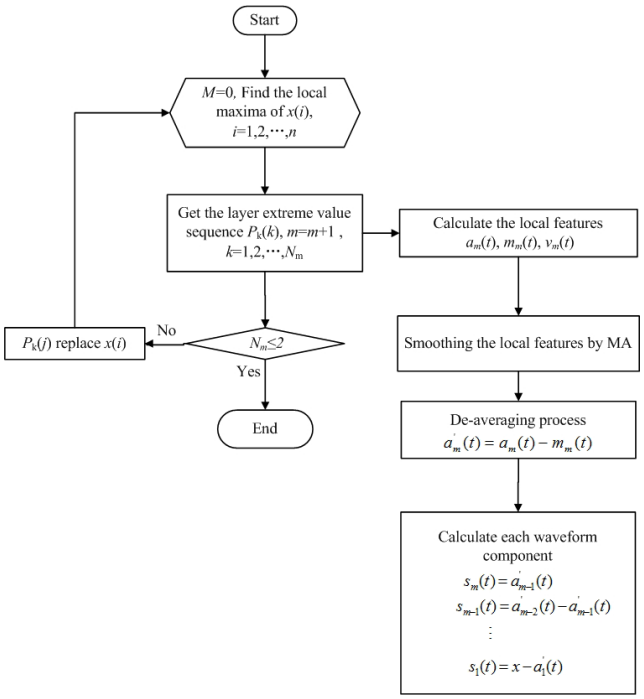

FIGURE 2. The flow chart of the AWD algorithm.

according to some simulation signal which have the similar feature of nonlinearity and non-stationarity with reciprocating compressor. Therefore, a simulation examples are taken as the research object, and the main characteristics of the proposed method above in the analysis of multi-component signals are detailed by being compared with the EMD (Empirical Model Decomposition) method [25]. In this way, we can easily justify the correctness of decomposition result by comparing with the original signal components. In the equation (10), the signal $x(t)$ consists of a harmonic signal and a FM-AM signal.

$$x(t) = \sin(2\pi \cdot 30t) + [1 + 0.5\sin(2\pi \cdot 10 \cdot t)] \cdot \cos[2\pi \cdot 150 \cdot t + 2\cos(2\pi \cdot 5 \cdot t)] \tag{10}$$

The decomposition effects of the simulation signal $x(t)$ based on AWD and EMD are shown in FIGURE 3. Obviously, both of them can effectively extract the three waveform component contained in the original signal, which are decomposed from high frequency to low frequency respectively. The figure suggests that the first layer of AWD and EMD result is the FM-AM component, the second layer is the harmonic component, and the third layer is the trend term. With the rise in the number of decomposition layers, the distance between the first extreme point of the layer and the first data point will increase. Whether it is the sliding average method or the spline envelope method, it is difficult to give a satisfactory fit. Though many scholars have given various end-point extension methods, these methods have always been ineffective for nonlinear and non-stationary signals. Accordingly, the proposed method is capable of accurately extracting the essential features of the waveform components contained

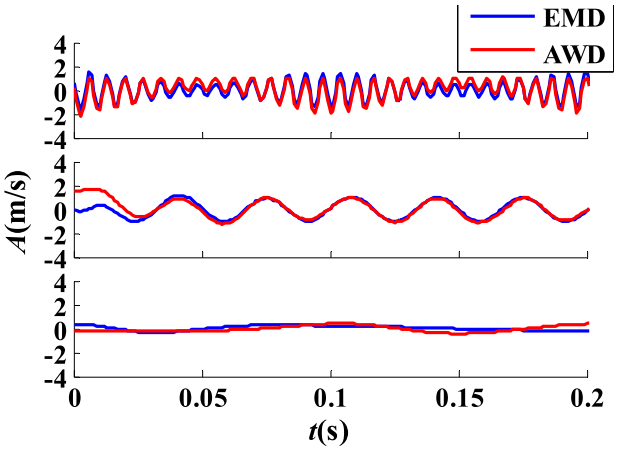

FIGURE 3. The decomposition result of the signal $x_2(t)$ based on AWD and EMD.

TABLE 1. Performance and structure parameters of the 2D12 compressor.

Name	Compressor	Type	2D12-70/0.1~1.3
First stage suction pressure	0.01 MPa	Motor type	JB500-12
Second stage exhaust pressure	1.3 MPa	Motor speed	496 r/min
Suction tempure	≤18 ℃	Connecting rod length	600 mm
Exhaust temperature	≤140 ℃	Piston stroke	240 mm
Displacement	70 m^3/h	Piston rod diameter	70 mm
First stage Cylinder diameter	690 mm	First stage Cylinder diameter	370 mm

in the original signal, and its validity and applicability was verified according to the simulation signal above.

C. EXPERIMENTAL ANALYSIS

In this study, a 2D12-70/0.1∼13 type reciprocating compressor was used for the experimental. The compressor consists of a two-stage air intensifier with an air-cooling system. A three-phase induction motor drives the compressor to run at a speed of 496 rpm. The details of the system are provided in TABLE 1 below.

For the experimental study, the compressor is instrumented with several different sensors. A pressure transducers are mounted into the second cylinder to measure the cylinder pressure waveforms. An optical shaft encoder is attached to the crankshaft. There are six vibration acceleration transducers fixed on gas valve cover as shown in FIGURE 4. Based on the experimental system, some experiments were carried out with four types of reciprocating compressor gas valves including normal valve, gap valve, fractured valve and bad spring valve. Sample frequency is 20000 Hz. FIGURE 5 displays the disposition of experimental equipment. The time waveforms of vibration for reciprocating compressor gas valve in four states are shown in FIGURE 6.

In FIGURE 6, due to the existence of faults, the impact waveforms and impact moments vary, the features of each

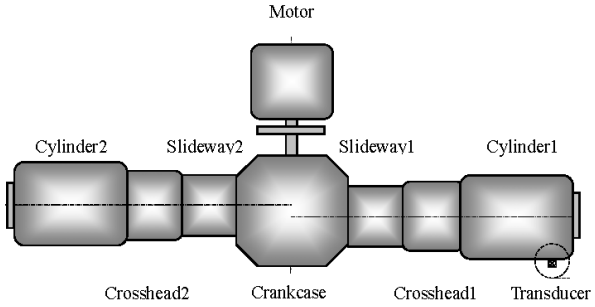

FIGURE 4. Measurement system of reciprocating compressor.

FIGURE 5. The disposition of experimental equipment for gas valve.

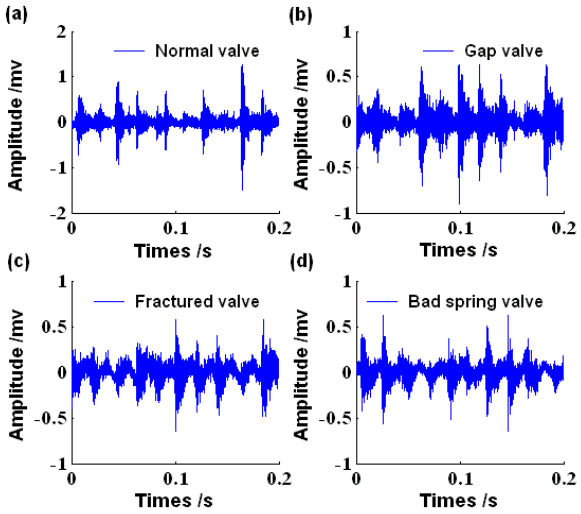

FIGURE 6. The time waveforms of gas valve in the four states.

time domain waveform are less significant, and even the feature of each cycle are difficult to judge. Thus, the excitation source corresponding to each impact waveform cannot be directly discriminated from the time domain waveform. To more effectively extract the time-domain features of the multi-source shock vibration signal of the reciprocating compressor, the AWD method proposed in this study was applied. Take the vibration signal in normal valve state as an example.

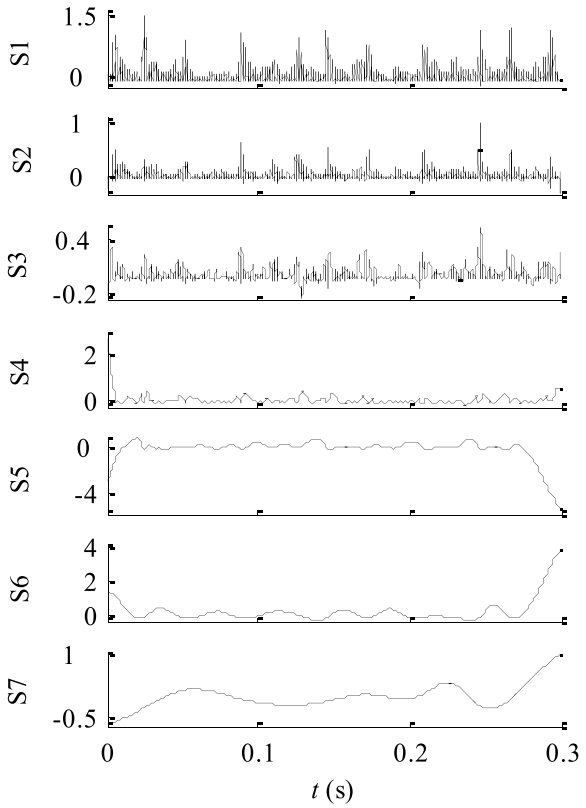

FIGURE 7. The AWD result of the vibration signal in the normal state of gas valve.

The AWD result of the vibration signal in the normal state of the gas valve is shown in FIGURE 7. The original signal was quickly decomposed into 7 waveform component signals, and it could be discriminated that the first three waveform components belong to the high frequency band signal, and the last four waveform components belong to the low frequency band. The signal was analyzed from the amplitude variation. With the rise in the number of decomposition layers, the smaller extremum information will be gradually filtered out, i.e. the larger extremum information will be retained, and the endpoint effect will be gradually increased.

The EMD result of the vibration signal in the normal state of gas valve is shown in FIGURE 8. At this time, the signal is split into 11 layers of IMF (Intrinsic Mode Function) components. The iteration speed is obviously slower than that of the AWD method, and the frequency also varied from high to low. The amplitude is gradually larger than that of decomposition layers, and the endpoint effect is inclined to be amplified as well. From the decomposition effect, the number of EMD decomposition layers is too small, the bandwidth between the layers may overlap, and the latter two layers exhibit poor signal volatility, which should belong to the trend item category. Redundant information are attributed to the strict convergence condition of EMD. In contrast, the AWD method exhibits higher decomposition efficiency, and the difference between layers is easy to recognize. The last

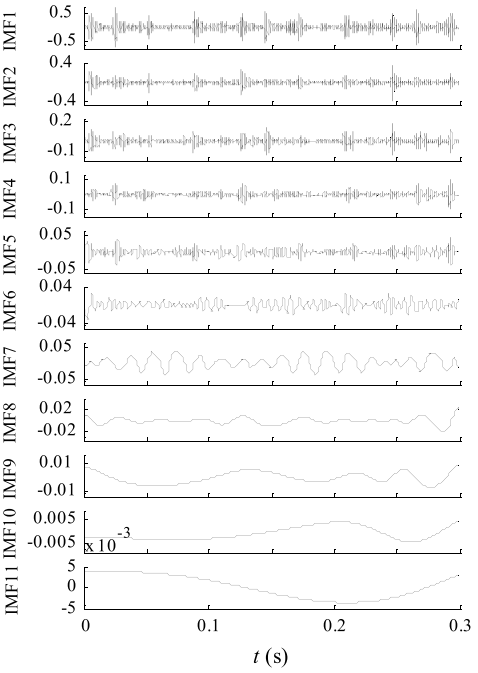

FIGURE 8. The EMD result of the vibration signal in the normal state of gas valve.

component is not a trend term but a signal component that still has a meaning of fluctuation. Accordingly, by comparing the time domain features of the two adaptive decomposition methods in the normal state of gas valve, it is revealed that the AWD method have better decomposition efficiency and decomposition effect than the EMD method.

IV. FEATURE EXTRACTION OF NONLINEAR TIME SERIES BASED ON LZC

A. ALGORITHM OF LZC

The definition of complex measure was proposed by Kolmogorov and characterized by the number of bits of the shortest program required to generate a sequence of symbols. Later, to achieve this complexity, A. Lempel and J. Ziv proposed an algorithm called Lempel-Ziv complexity (LZC), which has been widely used in nonlinear scientific research [26]. LZC analysis is based on a coarse-graining of the measurements. Before the LZC measure is calculated, the time series should be converted into a finite symbol sequence. In general, an arbitrary time series $\{x(i)|i = 1, 2, 3, \cdots, n\}$ is converted into a binary series. Compared with the threshold, $x(i)$ are converted into a 0–1 series $\{S(i)|i = 1, 2, 3, \cdots, n\}$ as follows [27].

$$S(i) = \begin{cases} 0 & x(i) < x_{ave} \\ 1 & x(i) \geq x_{ave} \end{cases} \tag{11}$$

where xave denotes the mean of time series of $x(i)$. Then, the LZC measure can be estimated using the following algorithm as shown in FIGURE 9.

Above algorithm is repeated until Q becomes the last character. The measure of complexity is $c(n)$. To obtain

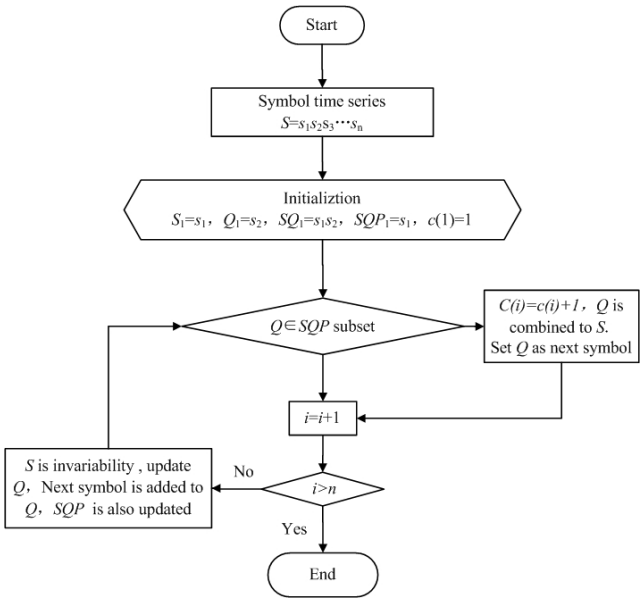

FIGURE 9. The principle diagram of LZC.

a complexity measure independent of the series length, $c(n)$ should be normalized. If the length of the sequence is n and the number of different symbols in the symbol set is 2, it has been proved that the upper bound of $c(n)$ is defined as

$$\lim_{n\to\infty} c(n) = b(n) = \frac{n}{\log_2(n)} \tag{12}$$

and c(n) can be normalized by b(n)

$$0 \le C = \frac{c(n)}{b(n)} \le 1 \tag{13}$$

where the normalized complexity index C is termed as Lempel-Ziv complexity.

Obviously, equation (13) can be established only if the sample length n is sufficiently large. The literature has given the experience valve $n \ge 3600$ [28] The complexity index C denotes the random degree of time series. For the completely random time series, C is close to 1. Furthermore, the periodic time series is close to 0. In practice, the vibration signals of reciprocating compressor vary with each fault states randomly, so the LZC can be extracted as a useful measure for machine health condition features.

B. PERFORMANCE EXPERIMENT OF LZC

To verify the effectiveness of LZC method, the typical nonlinear dynamical system were taken as an example to investigate the performance of LZC. Consider the following Logistic map [29]

$$x_{n+1} = \lambda \cdot x_n \cdot (1 - x_n), \tag{14}$$

where $x_n \in [0, 1]$, $\lambda \in [2.8, 4]$; λ is the control parameters; the step size is 0.01. The sample length of nonlinear time series is $N = 5000$.

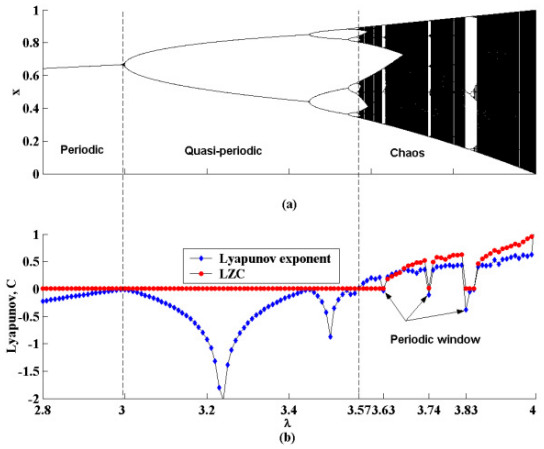

FIGURE 10. The Logistic map with different parameters λ. (a) Bifurcation diagram; (b) comparison of lyapunov exponent and LZC.

According to the LZC algorithm, the complexity index C of Logistic map with different parameters λ can be calculated; the result is shown in FIGURE 10.

Observe FIGURE 10(a) and FIGURE 10(b), it indicates the dynamical behavior of logistic map with different control parameters λ. The trends of Lyapunov exponent and the complexity index C are much synchronous. When $2.8 \le \lambda < 3.57$, Lyapunov exponent is less than zero and it shows that Logistic system enters in periodic or quasi-periodic region. Moreover, most values of LZC are close to zero. When $3.57 < \lambda \le 4$, Lyapunov exponent is greater than zero and it indicates that the system enters chaos region. In the meantime, the complexity index C tends to be around 0.5. During this region, Lyapunov exponent less than zero including $\lambda = 3.63$, $\lambda = 3.74$ and $\lambda = 3.83$ are called periodic windows. In these regions, the complexity index C is still close to zero.

In summary, LZC can be used as identifying the dynamical behavior of nonlinear system effectively. The analysis results are stable and reliable when the number of samples increase. Thus, the LZC value of different system states can be compared together without any prior knowledge about fault mechanism.

V. APPLICATION IN FAULT FEATURE EXTRACTION OF RECIPROCATING COMPRESSOR

A. PRE-PROCESSING ANALYSIS OF VIBRATION SIGNAL

To reduce the influence of noise on the nonlinear and non-stationary measure analysis results of multi-source impact signals of gas valve, the pre-processing based on AWD and mutual information (MI) fusion noise reduction technology was proposed. The definition of MI can be given as follow [30].

$$\begin{aligned} I(X, Y) &= H(X) + H(Y) - H(X, Y) \\ &= \sum_{i-1}^{n}\sum_{j-1}^{m} P(x_i, y_j) \log \frac{p(x_i, y_j)}{p(x_i)\, p(y_j)} \end{aligned} \tag{15}$$

where $p(x)$, $p(y)$ and $p(x, y)$ denote the probability density function of two random variables X, Y and the joint probability distribution of (X, Y). MI indicates whether the two variables X and Y have a relationship, and the strength of the relationship. When they are absolute, MI value will be 0. When they are fully the same, the value will be 1.

The vibration signal in the normal state of the gas valve was taken as an example to illustrate the process. As shown in FIGURE 7, the original valve signal is adaptively decomposed into 7 waveform component signals. $s_1, s_2, \cdots s_7$. The MI value of each component signal and the original signals were calculated following the steps of the equations (15), respectively, and the results are shown in FIGURE 11.

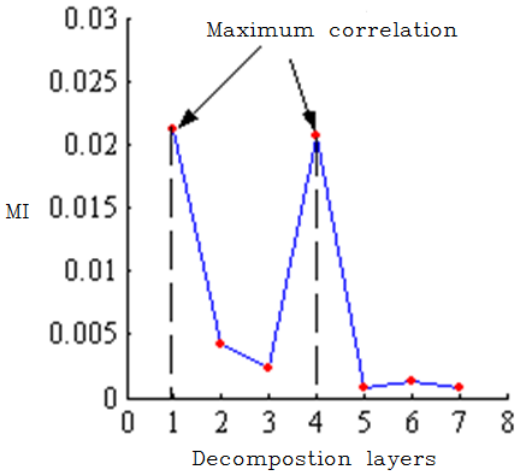

FIGURE 11. Mutual information between each component signal and the original valve vibration signal.

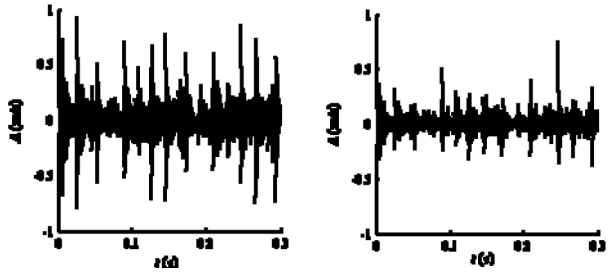

(a) Before noise reduction (b) After noise reduction

FIGURE 12. Comparison of noise reduction pretreatment results of gas valve normal state vibration signal.

FIGURE 11 shows that the MI values of the first layer and the fourth layer are the largest, which is significantly higher than the other layers. So it indicates that the correlation between the waveform component signals s1 and s4 and the original valve signal is the strongest. Accordingly, the two component signals are selected for recombination as the noise-reduced signal. FIGURE 12 shows the comparison of the effects before and after the noise reduction process. The noise-reduced signal maintains the periodic characteristics and impact characteristics of the original signal, and achieves the purpose of noise reduction, while retaining the characteristic information of the original valve vibration signal.

B. LZC ANALYSIS OF GAS VALVE VIBRATION SIGNAL

After the noise reduction pre-processing of the reciprocating compressor, the proposed LZC method is used to calculate the normalized LZC index of the valve signal in the four states. To improve the accuracy of the comparison results, each valve state is selected. For the 10 groups of samples, the sample length is selected as 10000, and the calculation result is shown in FIGURE 13.

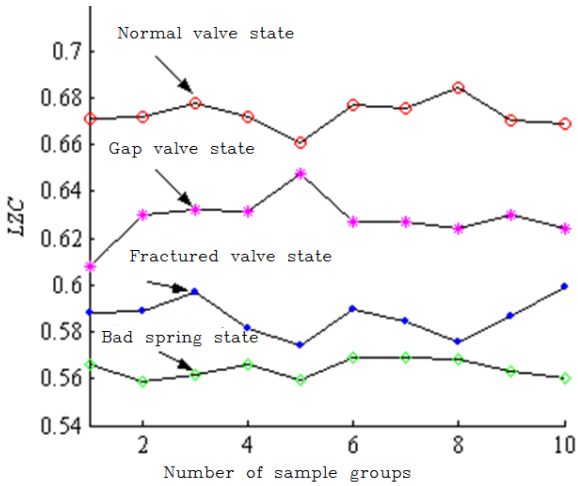

FIGURE 13. Comparison of vibration signals of LZC under different valve conditions.

TABLE 2. Time domain LZC interval division of vibration signals under different valve conditions.

Gas valve state	Mean / m	Variance / σ	Characteristic interval / (m-3σ, m+3σ)
Normal valve	0.6729	0.0060	(0.6548, 0.6910)
Gap valve	0.6283	0.0093	(0.6004, 0.6562)
Fractured valve	0.5865	0.0077	(0.5635, 0.6095)
Bad spring	0.5640	0.0038	(0.5526, 0.5755)

FIGURE 13 indicates that the normalized LZC index distinguishes the feature extraction effects of the reciprocating compressor valve signals in the four states, and there is no crossover interference. The LZC index values of different groups of samples in the same state are stable as well, following the statistical "3σ" principle: the closer the distance mean, the greater the probability of value will be; the smaller the opposite, the majority of the values will fall on $(m - 3\sigma, m + 3\sigma)$ within the interval. The LZC indicator characteristic value interval of each state of the reciprocating compressor valve can be split, as listed in TABLE.2. Though the LZC index has small crossover and overlap in each state

of the gas valve, it is a small probability event according to the probability "3σ" principle.

C. DYNAMIC LZC FEATURE

To verify the reliability and repeatability of the LZC index partition interval, a dynamic LZC algorithm was proposed: for a time series of length N, from the first data, the data in the rectangular window of length L is sub- Sequence, LZC processing is normalized, and then the window is slid backwards; the sliding step is τ points, the next set of sub-sequences is obtained, thus $(N-L)/\tau$ LZC indicators are obtained, forming a group with time. The dynamic LZC indicator of variation not only considers the global basic features of the signal, but also extracts local detail features. The length of the sample is $N = 200000$, the length of the window is $L = 10000$, and the size of sliding step is $\tau = 2000$. The LZC sequence of 95 sets of data samples can be developed. The evolution curve of each state LZC with time is shown in FIGURE 14.

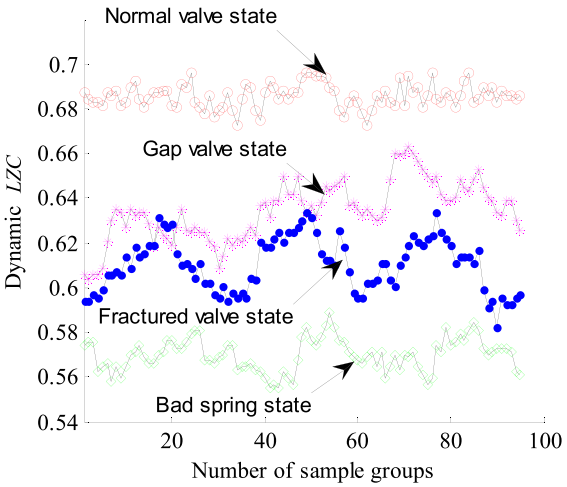

FIGURE 14. Dynamic LZC comparison of vibration signals under different valve conditions.

FIGURE 14 suggests that the LZC index of each state is more obvious, in which the LZC value of the gas valve is the largest under normal state, followed by the valve plate notch state and the valve less spring state. From the perspective of time volatility, the fluctuation of the gas valve under normal conditions is the smallest, followed by the valve less spring state and the valve plate notch state; the fluctuation of the valve plate in the fracture state is the largest. Most of the state LZC indicators still fall within the division range of the state, and the coincidence rate is over 95%, suggesting that the LZC index does not change significantly due to the change of sample points. It exhibits good stability and recognition ability, and it is of certain reference implication for gas valve fault diagnosis.

VI. CONCLUSION

An integrated method based on AWD and LZC was proposed to achieve feature extraction for the vibration signal of reciprocating compressor with nonlinear and non-stationary characteristics. According to the AWD, the multi-component signal can be converted into a series single-component signal adaptively without any prior-knowledge. The LZC feature interval exhibits good reliability and repeatability, capable of effectively identifying different states of the reciprocating compressor. Over time, the dynamic LZC index in different states is reflected in the complexity and randomness evolution of the state of the reciprocating compressor system. The fluctuation of the gas valve under normal conditions is the smallest, and the stability is the best. Subsequently, the spring is damaged, the valve plate is notched, and the valve plate exhibits the largest fluctuation and the worst stability.

DATA AVAILABILITY

The data used to support the findings of this study are included within the article.

CONFLICTS OF INTEREST

The authors declare that there are no conflicts of interest regarding the publication of this paper.

REFERENCES

[1] S. Xiao, S. Liu, F. Jiang, M. Song, and S. Cheng, "Nonlinear dynamic response of reciprocating compressor system with rub-impact fault caused by subsidence," *J. Vib. Control*, vol. 25, no. 11, pp. 1737–1751, 2019.
[2] Z. Haiyang, W. Jindong, J. Lee, and L. Ying, "A compound interpolation envelope local mean decomposition and its application for fault diagnosis of reciprocating compressors," *Mech. Syst. Signal Process.*, vol. 110, pp. 273–395, Sep. 2018.
[3] Z. Hai-Yang, X. Min-Qiang, W. Jin-Dong, and L. Yong-Bo, "A parameters optimization method for planar joint clearance model and its application for dynamics simulation of reciprocating compressor," *J. Sound Vib.*, vol. 344, pp. 416–433, May 2015.
[4] F. Balduzzi, A. Tanganelli, G. Ferrara, and A. Babbini, "Two-dimensional approach for the numerical simulation of large bore reciprocating compressors thermodynamic cycle," *Appl. Thermal Eng.*, vol. 129, pp. 490–501, Jan. 2018.
[5] Y.-F. Tang and S.-L. Li, "Time-frequency feature extraction from multiple impulse source signal of reciprocating compressor based on local frequency," *J. Vibroeng.*, vol. 15, no. 2, pp. 574–587, 2013.
[6] F. J. Harris, "On the use of windows for harmonic analysis with the discrete Fourier transform," *Proc. IEEE*, vol. 66, no. 1, pp. 51–83, Jan. 1978.
[7] D. Griffin and J. Lim, "Signal estimation from modified short-time Fourier transform," *IEEE Trans. Acoust., Speech, Signal Process.*, vol. ASSP-32, no. 2, pp. 236–243, Apr. 1984.
[8] I. Daubechies, "The wavelet transform, time-frequency localization and signal analysis," *IEEE Trans. Inf. Theory*, vol. 36, no. 5, pp. 961–1005, Sep. 1990.
[9] J. Wang, Q. Wei, L. Zhao, T. Yu, and R. Han, "An improved empirical mode decomposition method using second generation wavelets interpolation," *Digit. Signal Process.*, vol. 79, pp. 164–174, Aug. 2018.
[10] S. Mouatadid, J. F. Adamowski, M. K. Tiwari, and J. M. Quilty, "Coupling the maximum overlap discrete wavelet transform and long short-term memory networks for irrigation flow forecasting," *Agricult. Water Manage.*, vol. 219, pp. 72–85, Jun. 2019.
[11] J. Wang, Y. Han, L. M. Wang, P. Z. Zhang, and P. Chen, "Instantaneous frequency estimation for motion echo signal of projectile in bore based on polynomial chirplet transform," *Russian J. Nondestruct. Test.*, vol. 54, no. 1, pp. 44–54, 2018.
[12] J. Tan, "Atomic decomposition of variable Hardy spaces via Littlewood–Paley–Stein theory," *Ann. Funct. Anal.*, vol. 9, no. 1, pp. 87–100, 2018.
[13] N. E. Huang, Z. Shen, S. R. Long, M. C. Wu, H. H. Shih, Q. Zheng, N.-C. Yen, C. C. Tung, and H. H. Liu, "The empirical mode decomposition and the Hilbert spectrum for nonlinear and non-stationary time series analysis," *Proc. Roy. Soc. London A, Math., Phys. Eng. Sci.*, vol. 454, no. 1971, pp. 903–995, Mar. 1998.

[14] J. S. Smith, "The local mean decomposition and its application to EEG perception data," *J. Roy. Soc. Interface*, vol. 2, no. 5, pp. 443–454, 2005.
[15] J. S. Cheng, J. D. Zheng, and Y. Yang, "A nonstationary signal analysis approach-The local characteristic-scale decomposition method," *J. Vibrat. Eng.*, vol. 25, no. 2, pp. 215–220, 2012.
[16] D. Faranda and S. Vaienti, "Correlation dimension and phase space contraction via extreme value theory," *Chaos, Interdiscipl. J. Nonlinear Sci.*, vol. 28, no. 4, 2018, Art. no. 041103.
[17] M. L. C. Peixoto, E. G. Nepomuceno, S. A. M. Martins, and M. J. Lacerda, "Computation of the largest positive Lyapunov exponent using rounding mode and recursive least square algorithm," *Chaos, Solitons Fractals*, vol. 122, pp. 36–43, Jul. 2018.
[18] N. Arunkumar, K. Ram Kumar, and V. Venkataraman, "Automatic detection of epileptic seizures using permutation entropy, Tsallis entropy and Kolmogorov complexity," *J. Med. Imag. Health Inform.*, vol. 6, no. 2, pp. 526–531, 2016.
[19] H. Zenil, S. Hernández-Orozco, N. Kiani, F. Soler-Toscano, A. Rueda-Toicen, and J. Tegnér, "A decomposition method for global evaluation of Shannon entropy and local estimations of algorithmic complexity," *Entropy*, vol. 20, no. 8, p. 605, 2018.
[20] T. Bansal, G. S. Haji, H. B. Rossiter, M. I. Polkey, and J. H. Hull, "Exercise ventilatory irregularity can be quantified by approximate entropy to detect breathing pattern disorder," *Respiratory Physiol. Neurobiol.*, vol. 255, pp. 1–6, Sep. 2018.
[21] A. Porta, V. B. B. De Maria, B. Cairo, E. Vaini, M. Malacarne, M. Pagani, and D. Lucini, "On the relevance of computing a local version of sample entropy in cardiovascular control analysis," *IEEE Trans. Biomed. Eng.*, vol. 66, no. 3, pp. 623–631, Mar. 2019.
[22] X. Li, Z. Zhu, W. Zhao, Y. Sun, D. Wen, Y. Xie, X. Liu, H. Niu, and Y. Han, "Decreased resting-state brain signal complexity in patients with mild cognitive impairment and Alzheimer's disease: A multi-scale entropy analysis," *Biomed. Opt. Express*, vol. 9, no. 4, pp. 1916–1929, 2018.
[23] K. Yu, J. Tan, and T. Lin, "Fault diagnosis of rolling element bearing using multi-scale Lempel–Ziv complexity and Mahalanobis distance criterion," *J. Shanghai Jiaotong Univ. (Sci.)*, vol. 23, no. 5, pp. 696–701, 2018.
[24] G. Qi, Z. Zhu, K. Erqinhu, Y. Chen, Y. Chai, and J. Sun, "Fault-diagnosis for reciprocating compressors using big data and machine learning," *Simul. Model. Pract. Theory*, vol. 80, pp. 104–127, Jan. 2018.
[25] X. Mi, H. Liu, and Y. Li, "Wind speed prediction model using singular spectrum analysis, empirical mode decomposition and convolutional support vector machine," *Energy Convers. Manage.*, vol. 180, pp. 196–205, Jan. 2019.
[26] A. Lempel and J. Ziv, "On the complexity of finite sequences," *IEEE Trans. Inf. Theory*, vol. IT-22, no. 1, pp. 75–81, Jan. 1976.
[27] J. Ziv and A. Lempel, "A universal algorithm for sequential data compression," *IEEE Trans. Inf. Theory*, vol. IT-23, no. 3, pp. 337–343, May 1977.
[28] H. Hong and M. Liang, "Fault severity assessment for rolling element bearings using the Lempel–Ziv complexity and continuous wavelet transform," *J. Sound Vibrat.*, vol. 320, nos. 1–2, pp. 452–468, 2009.
[29] S. C. Phatak and S. S. Rao, "Logistic map: A possible random-number generator," *Phys. Rev. E, Stat. Phys. Plasmas Fluids Relat. Interdiscip. Top.*, vol. 51, no. 4, p. 3670, 1995.
[30] M. Koch-Janusz and Z. Ringel, "Mutual information, neural networks and the renormalization group," *Nature Phys.*, vol. 14, no. 6, pp. 578–582, 2018.

YOUFU TANG received the master's degree from the Mechanical Science and Engineering College, Northeast Petroleum University, China, in 2006, and the Ph.D. degree in mechanical and electronic engineering from the School of Mechatronic Engineering and Automation, Shanghai University, China, in 2013. He is currently an Associate Professor in engineering mechanics with the Mechanical Science and Engineering College, Northeast Petroleum University. His current research interests include mechanical fault diagnosis, noise, and vibration control.

FENG LIN received bachelor's degree from the Information Engineering College, West Anhui University, in 2017. He is currently pursuing the master's degree with the Mechanical Science and Engineering College, Northeast Petroleum University, China. His current research interests include pattern recognition, mechanical fault diagnosis, and vibration control.